

Lawrence Berkeley National Laboratory

Lawrence Berkeley National Laboratory

Title

ForCent model development and testing using the Enriched Background Isotope Study experiment

Permalink

<https://escholarship.org/uc/item/1wn7j1f0>

Author

Parton, W.J.

Publication Date

2010-12-01

DOI

DOI: 10.1029/2009jg001193.

Peer reviewed

1 **Running Head:** ForCent Model Development using the Enriched Background Isotope Study

2

3

ForCent Model Development and Testing using the

4

Enriched Background Isotope Study Experiment

5

6 William J. Parton¹, Paul J. Hanson², Chris Swanston³, Margaret Torn⁴, Susan E. Trumbore⁵,

7 William Riley⁴, Robin Kelly¹

8

9 **Corresponding author:** William J. Parton

10 Natural Resource Ecology Laboratory, Colorado State University

11 Fort Collins, CO 80523-1499

12 Phone: (970) 491-1987; Fax: (970) 491-1965

13 E-mail: billp@nrel.colostate.edu

14

¹ Natural Resource Ecology Laboratory, Colorado State University, Fort Collins, Colorado, USA

² Oak Ridge National Laboratory, Oak Ridge, Tennessee, USA

³ USFS, Northern Research Station, Houghton, Michigan, USA

⁴ Lawrence Berkeley National Laboratory, Berkeley, California, USA

⁵ School of Physical Sciences, University of California, Irvine, California, USA

15 **Abstract**

16 The ForCent forest ecosystem model was developed by making major revisions to the
17 DayCent model including: 1) adding a humus organic pool, 2) incorporating a detailed root
18 growth model, and 3) including plant phenological growth patterns. Observed plant production
19 and soil respiration data from 1993-2000 were used to demonstrate that the ForCent model could
20 accurately simulate ecosystem carbon dynamics for the Oak Ridge National Laboratory
21 deciduous forest. A comparison of ForCent vs. observed soil pool ^{14}C -signature ($\Delta^{14}\text{C}$) data
22 from the Enriched Background Isotope Study ^{14}C experiment (1999-2006) shows that the model
23 correctly simulates the temporal dynamics of the ^{14}C label as it moved from the surface litter and
24 roots into the mineral soil organic matter pools. ForCent model validation was performed by
25 comparing the observed Enriched Background Isotope Study experimental data with simulated
26 live and dead root biomass $\Delta^{14}\text{C}$ data, and with soil respiration $\Delta^{14}\text{C}$ (mineral soil, humus layer,
27 leaf litter layer, and total soil respiration) data. Results show that the model correctly simulates
28 the impact of the Enriched Background Isotope Study ^{14}C experimental treatments on soil
29 respiration $\Delta^{14}\text{C}$ values for the different soil organic matter pools. Model results suggest that a
30 two-pool root growth model correctly represents root carbon dynamics and inputs to the soil. The
31 model fitting process and sensitivity analysis exposed uncertainty in our estimates of the fraction
32 of mineral soil in the slow and passive pools, dissolved organic carbon flux out of the litter layer
33 into the mineral soil, and mixing of the humus layer into the mineral soil layer.

34

35 **Index Terms:** 0400 Biogeosciences; 0428 Carbon cycling (4806); 0439 Ecosystems, structure
36 and dynamics (4815); 0466 Modeling (1952); 0486 Soils/pedology (1865)

37
38 **Key Words:** Modeling, Soil carbon, Soil $\Delta^{14}\text{C}$, Litter decomposition, Century, ForCent

39

40 **1. Introduction**

41 Decomposition of root and leaf litter is a critical process for releasing soil nutrients for plant
42 growth and for providing substrate for the formation of soil organic matter. This process is
43 included in all of the major ecosystem models [see Century: *Parton et al.*, 1987; Biome-BGC:
44 *Running and Coughlan*, 1988; DNDC: *Li et al.*, 1994; Roth-C: *Coleman and Jenkinson*, 1996].
45 Root and leaf litter substrate is incorporated into soil organic matter pools with rapid,
46 intermediate, and slow turnover times. The conceptual development of these pools was based on
47 studies of the impact of root and leaf litter decay on soil organic matter levels and nutrient
48 dynamics [*Meentemeyer*, 1978; *Melillo et al.*, 1982; *Hobbie*, 1996; *Parton et al.*, 2007a].

49 The most common technique for studying these decomposition dynamics is to use litter bags
50 [reviewed in *Wieder and Lang*, 1982; *Parton et al.*, 2007a]. Most litter bag studies have been run
51 for relatively short time periods [three years or less: *Shanks and Olson*, 1961; *Lousier and*
52 *Parkinson*, 1976; *McClaugherty et al.*, 1985; *Aerts et al.*, 2003]; however, a few studies were run
53 for a longer period time (five or more years: *Trofymow et al.*, 2002; *Parton et al.*, 2007a). Results
54 from the long-term studies suggest that 5-20% of the initial litter plant biomass is stabilized into
55 the slow turnover soil organic matter pool. The recent global litter decay study by Parton et al.,
56 (2007a) showed photodegradation can greatly enhance surface litter decay rates for dry grassland
57 ecosystems; however, photodegradation does not seem to be an important process for humid
58 grasslands and forest ecosystems. The major limitation of litter bag techniques, however, is that

59 they do not directly evaluate the subsequent fate of nutrients and organic matter released from
60 litter bags [see *Dornbush et al.*, 2002].

61 A number of studies using isotopic tracers (^{13}C and ^{14}C) have been conducted to address gaps
62 in the scientific knowledge of the relationships between litter decomposition and the formation
63 of soil organic matter [*Jenkinson*, 1971; *Wang et al.*, 1996]. Since the isotopic signature of soil
64 organic matter is similar to the vegetation system under which it was formed, a difference in
65 plant vs. soil $\Delta^{13}\text{C}$ suggests a relatively recent change in plant cover. Isotopic approaches have
66 been used to track changes in ecotone boundaries [*Steuter et al.*, 1990; *McClaran and*
67 *McPherson*, 1995], detect land use conversion from tropical C_3 -dominated forests to C_4 -
68 dominated cropping systems [*Osher et al.*, 2003]. Estimates of the minimum age of a soil organic
69 matter pool or the mean residence time of the organic material are possible using ^{14}C -dating
70 [*Paul et al.*, 1997], and may be used to track changes in slow and passive soil organic matter.
71 Both ^{13}C - and ^{14}C -signatures ($\Delta^{13}\text{C}$ and $\Delta^{14}\text{C}$, respectively) are used to track litter
72 decomposition and soil organic matter formation and stabilization [*Follett et al.*, 2007]. The
73 results from these studies support the three-pool soil organic matter structure common in
74 ecosystem soil C cycle models.

75 This paper describes the use of the Enriched Background Isotope Study $\Delta^{14}\text{C}$ [*Hanson et al.*,
76 2005] litter and root experiments to calibrate, develop, and test a mechanistically improved forest
77 version of the DayCent model (ForCent). The main objective of this paper is to determine how
78 well the extensive Enriched Background Isotope Study $\Delta^{14}\text{C}$ data sets can be used to determine
79 the turnover rates of the different soil organic matter pools using a process-based ecosystem
80 model. We utilized the classic modeling approach by using part of the observed data to develop
81 the new model and then selected a segment of the observed data to perform a true model

82 validation. A detailed description of the new ForCent model, the procedure used to calibrate the
83 model, limitations of the ForCent model, and a comparison of the model results with the
84 observed data sets are also presented. In addition, we included a sensitivity analysis of the model
85 to the assumed atmospheric $\Delta^{14}\text{C}$ values and the fraction of mineral soil carbon in slow and
86 passive fractions.

87 The ForCent model described here is better poised to address outstanding issues in the
88 terrestrial carbon cycle, including: (1) the partitioning of soil carbon turnover between
89 autotrophic and heterotrophic sources, (2) the partitioning of heterotrophic respiration sources
90 between above-ground litter decomposition and below-ground root detritus decomposition, and
91 (3) the clarification of pathways leading from leaf and root detritus to long-term stabilization of
92 soil organic matter. By incorporating a new understanding of important forest carbon cycling
93 pools and processes, ForCent is better prepared to address questions such as the influence of
94 climatic change on the longevity of new carbon additions to soils and the fate of long-lived
95 storage pools through time.

96

97 **2. Methods**

98 **2.1. The Enriched Background Isotope Study**

99 The Enriched Background Isotope Study project [*Trumbore et al.*, 2002; *Hanson et al.*, 2005;
100 *Swanston et al.*, 2005] started in the fall of 2000 on the U.S. Department of Energy's National
101 Environmental Research Park near Oak Ridge, Tennessee. The Enriched Background Isotope
102 Study plots are located on ridge-top and up-slope positions which are dominated by oak forests
103 that range in age from 65 to 150 years. Available aerial photographs show that the Enriched
104 Background Isotope Study sites are located on the east branch of the watershed which had a

105 closed canopy forest cover in 1935. The exact date for a prior clear-cut disturbance for the
106 Enriched Background Isotope Study plots is not exactly known; however, the state of the forest
107 in 1935 suggests that forest regrowth started after a 1900 clear cut. The experimental sites
108 included two soil types and two levels of ^{14}C exposure in 1999. Reciprocal transplants of
109 enriched vs. near-background litter were established on sites that had large (western site) and
110 minimal (east site) exposure to enhanced atmospheric levels of ^{14}C in 1999. Enriched ^{14}C leaf
111 litter was collected from the western site during the fall of 2000, while background ^{14}C litter was
112 collected from the eastern site during the same time period. Near background and enriched ^{14}C
113 leaf litter were added to the plots in May 2001, with continued additions of elevated and ambient
114 leaf litter (during winter months) for the next two years. Plots in the replicated experimental
115 design included those with: 1) ^{14}C enriched soil carbon, root litter, and leaf litter; 2) ^{14}C enriched
116 roots, soil carbon, and near background leaf litter; 3) near-background roots, soil carbon, and
117 elevated ^{14}C leaf litter; and 4) near background leaf litter, roots, and soil carbon. The ^{14}C content
118 of surface litter, humus, mineral soil layers, and soil respiration rates were measured from 2001
119 to 2005. As of 2004, natural background ^{14}C leaf litter was allowed to fall into the treatment
120 plots.

121 Atmospheric ^{14}C levels elevated during the aboveground testing of nuclear weapons have
122 been used as a tracer for the interpretation of biological carbon pathways for many years;
123 however, that tracer is now returning to pre-bomb levels limiting the sensitivity of such
124 observations [Swanston et al., 2005]. The local and unexpected enrichment of background ^{14}C on
125 the Oak Ridge Reservation provided a unique opportunity to address soil carbon cycling at
126 annual and even sub-annual time scales allowing for the direct testing of soil carbon cycle

127 mechanisms in forests at previously unresolved time intervals [*Trumbore et al.*, 2002; *Froberg et*
128 *al.*, 2007].

129

130 **2.2. DayCent Model Description**

131 The DayCent model [*Kelly et al.*, 2000; *DelGrosso et al.*, 2001a, 2001b; *Parton et al.*, 2001]
132 is the daily version of the Century model [*Parton et al.*, 1987] developed to simulate daily trace
133 gas fluxes (CO₂, N₂O, NO_x, CH₄, N₂) from ecosystems. The objective was to develop a model
134 capable of simulating full greenhouse gas fluxes and net ecosystem exchange of carbon for
135 agricultural systems, grasslands, savanna, and forest systems. The model has been used
136 extensively to simulate the ecosystem dynamics of grasslands and forest and cropping systems in
137 the U.S. [*Kelly et al.*, 2000; *DelGrosso et al.*, 2001a; *DelGrosso et al.*, 2005]. *DelGrosso et al.*
138 [2005] recently used the DayCent model to simulate the impact of agricultural management
139 practices on soil carbon levels, trace gas fluxes, and crop yields for agricultural systems in the
140 U.S. at site, regional, and national levels. The DayCent model has also been used to simulate the
141 impact of nitrogen deposition, changing CO₂ levels, and future climatic changes [*Pepper et al.*,
142 2005; *Parton et al.*, 2007b; *Luo et al.*, 2008] on grassland and forest systems. The model
143 simulates soil nutrients (N and P) and carbon dynamics, trace gas fluxes (N₂O, NO_x, N₂, and
144 CH₄), plant production and nutrient uptake, and soil water and temperature dynamics (Figure 1).
145 The DayCent model uses a daily time step to simulate trace gas fluxes and soil nutrient and
146 carbon dynamics, one half hour time for the soil water flow, and daily time step for the plant
147 production submodel.

148 The plant production submodel simulates the growth of forests, grasslands, and savanna
149 systems. Important processes represented in the plant growth submodel include plant death, plant

150 phenology, uptake of soil nutrients, and growth of different plant parts. The factors controlling
151 plant growth are daily solar radiation, soil water and temperature, live leaf area, and soil nutrient
152 uptake by plants. A detailed description of the plant growth submodel is presented by *Kelly et al.*
153 [2000] and *DelGrosso et al.* [2001a]. The plant growth model simulates dynamic allocation of
154 carbon to the different plant parts as a function of water and nutrient stress. This paper presents a
155 detailed description of the most recent changes to the forest plant growth submodel.

156 The soil temperature and water submodels simulate daily soil temperature and water content
157 for the soil layers represented in the model. The soil temperature model is described by *Eitzinger*
158 *et al.* [2000], while *Parton et al.* [1998] present a detailed description of the soil water model.
159 The soil water model simulates saturated and unsaturated water flow, surface runoff, and deep
160 drainage below the plant rooting zone. Darcy water flow equations are used to simulate water
161 flow between soil layers using a one-half hour time step. Anaerobic conditions resulting from
162 snow melt into frozen soil layers are represented in the model. Soil temperatures are simulated
163 for each 5 cm depth increment using an analytical solution to the soil heat flow equations. The
164 soil temperature and water models have been tested extensively [*Frolking et al.*, 1998; *Eitzinger*
165 *et al.*, 2000; *DelGrosso et al.*, 2001a].

166

167 **2.3. ForCent model changes**

168 The major changes to the ForCent model include: 1) adding a surface litter slow organic
169 matter pool (humus layer); 2) altering the surface litter decay submodel; 3) adding the *Parton et*
170 *al.* [1978] root growth model; 4) adding a plant stored carbohydrate pool, and 5) including the
171 impact of phenology on seasonal plant growth patterns. The ForCent model divided the slow
172 pool into a surface slow pool (humus) and a mineral soil slow pool (see Figure 2). The need for

173 this change was emphasized by *Kelly et al.* [1997]. As part of this change, we added a flow that
174 simulates the physical mixing of the humus layer into the soil mineral slow pool. The surface
175 litter layer corresponds to the sum of the Century surface litter pools (structural and metabolic
176 pools) and the surface microbial biomass pool.

177 The *Riley et al.* [2009-Radix 1.0] and *Parton et al.* [1978] root growth models assume that
178 live fine roots are composed of roots with fast and slow turnover rates. The roots with fast
179 turnover rates are called juvenile roots, and roots with slow turnover rates are called mature
180 roots. *Riley et al.* [2009] suggest that juvenile roots have turnover times < 1.0 year, while mature
181 roots have turnover times > 10.0 years. The ForCent model has incorporated a revised version of
182 the *Parton et al.* [1978] root growth model (Figure 3). The main structural change for the
183 ForCent root model was to combine the juvenile and non-suberized roots into juvenile roots, and
184 then refer to the suberized roots as mature roots. The major process included in the *Parton et al.*
185 [1978] model includes maintenance respiration, growth of new roots, aging of juvenile roots, and
186 root death. Root maintenance respiration and root death are calculated as a function of soil water
187 content of the wettest layer and soil temperature, while aging of roots is a function of soil
188 temperature. The impacts of soil water and temperature on these processes are represented using
189 the *Parton et al.* [1978] model, while the maximum rates for root aging and root death were
190 parameterized based on the live root biomass data from the Enriched Background Isotope Study
191 [*Joslin et al.* 2006].

192 The revised model uses the original Century equations [*Parton et al.*, 1987] to control litter
193 decay for the soil pools (structural and metabolic dead roots, soil microbial biomass, and slow
194 and passive soil organic matter) within the mineral soil layer. Surface litter decay rates are now a

195 function of time since rainfall, average soil surface temperature, and soil water content of the 0-4
196 cm soil layer using equation 1:

$$197 \quad D_i = K_i * B_i * R * F(T_s) * F(w) \quad (1)$$

198 where D_i is the decomposition rate ($\text{g C m}^{-2} \text{d}^{-1}$) of i th soil pool ($i = 1, 2, 3,$ and 4 for the surface
199 metabolic, structural, microbial and humus pools), K_i is the maximum decay rate (d^{-1}) for the i th
200 surface litter pool, B_i is the carbon level (g C m^{-2}) in the i th surface litter pool, R is the rainfall
201 event multiplier (set equal to 1.0 for no precipitation days and 3.0 for days when precipitation is
202 > 10.0 mm), $F(T_s)$ is the impact of temperature on decomposition (Figure 4a), and $F(w)$ is the
203 effect of soil water on litter decay (Figure 4b). The same temperature and water functions are
204 used to simulate decay rates for the soil mineral pools (R is not used for the mineral soil pools).
205 Continuous soil respiration data from the Oak Ridge National Laboratory [*Hanson et al.*, 2005]
206 show that soil respiration rates from the surface litter increase rapidly following rainfall events
207 and then decrease as the soil litter dries out (generally within 24 to 36 hours).

208 The ForCent model includes a stored carbohydrate pool and currently assumes that gross
209 photosynthesis is equal to two times the net plant growth rates [*Waring et al.*, 1998; *DeLucia et*
210 *al.*, 2007; *Litton et al.*, 2007]. It predicts potential net plant growth rates as a function of air
211 temperature, water stress, and light interception, and then reduces these rates if nutrients are not
212 available. Stored carbohydrate is used to support growth of new leaves in the spring, with 50% of
213 new leaf growth coming from this pool. Carbon in the stored carbohydrate pool is the source for
214 growth and maintenance respiration. The model assumes that growth respiration is equal to
215 23.3% of the total growth of the different plant parts [*Hanson et al.*, 2003a], while maintenance
216 respiration rates are calculated using a model developed by *Ryan et al.* [1995] for live leaves,
217 branches, coarse roots, and stems. The Ryan respiration model assumes that each plant part has a

218 specific respiration rate and uses an exponential function to represent the effect of temperature
219 on maintenance respiration ($Q_{10} = 2.0$). The ForCent model assumes that maintenance respiration
220 rates are decreased if the carbohydrate pool is less than two times the maximum leaf carbon
221 level. We also assume that the stored carbohydrate pool will not exceed five times the maximum
222 leaf carbon level (carbon inputs to the stored carbohydrate are set equal to zero if the maximum
223 level is exceeded). The assumption regarding the maximum level for stored carbohydrate pools is
224 based on the concept that photosynthesis rates decrease if plant carbohydrate levels are too high,
225 while low levels of stored carbohydrates reduce maintenance respiration.

226 The ForCent model includes a dynamic carbon allocation scheme which assumes that fine
227 root growth has first priority, followed by live leaves and wood growth. The plant growth model
228 calculates the maximum plant growth rate as a function of air temperature, intercepted solar
229 radiation, and water stress [*Parton et al.*, 2001]. The model calculates the fraction of plant
230 production going to fine root growth (Fr) as a function of the water and nutrient stress using
231 equation 2:

$$232 \quad Fr = \text{maximum} (F (Ws), F (Ns)) \quad (2)$$

233 where $F (Ws)$ is the impact of water stress on Fr (increases linearly from 0.05 to 0.18 as water
234 stress increases from the minimum value to the maximum value) and $F (Ns)$ is the impact of
235 nutrient stress on Fr (increases linearly from 0.05 to 0.18 as nutrient stress increases from the
236 minimum value to the maximum value). The ratio of available nitrogen to plant nitrogen demand
237 is used as the index for nutrient stress (ratio equal to one is associated with minimum nutrient
238 stress), while the water stress term comes from the plant growth model. Fine root growth occurs
239 during the time periods when net plant production is positive and during the first month of spring
240 leaf out using the stored carbohydrate pool.

241 Live leaf growth receives the remaining carbon and nutrients available for plant growth until
242 the maximum live leaf area is attained. Maximum leaf area is specified for each plant type as a
243 function of the aboveground wood biomass using an allometric function. Wood growth occurs
244 after maximum leaf area is attained using the remaining available carbon and nutrients for wood
245 growth. The model specifies the fraction of carbon promoting wood growth in various plant parts
246 (20%, 65%, and 15% respectively for fine branches, large wood and coarse roots). Wood growth
247 is assumed to occur during the first four months following spring leaf out. The plant phenology
248 rules are based on Oak Ridge site data showing that maximum leaf area is attained a month after
249 spring leaf out starts and that new wood growth starts after maximum leaf area is attained, but
250 before the end of July. Initiation of spring leaf out starts after the weekly running average air
251 temperature exceeds 10° C and leaf senescence occurs after the weekly running average air
252 temperature drops below 7° C.

253

254 **2.4. The Enriched Background Isotope Study Computer Runs**

255 The ForCent model was set up to simulate the Enriched Background Isotope Study
256 experiments by running the model to equilibrium conditions using a 1900-year computer
257 simulation that used observed daily weather data (1900-2005) and soil texture data as inputs to
258 the model. In 1900, the forest was clear cut and then started to re-grow. The ecosystem dynamics
259 from 1900 to the present were simulated using the observed weather data from that time period.
260 The Enriched Background Isotope Study model experiments for the east and west sites were
261 started in 1995. The atmospheric $\Delta^{14}\text{C}$ levels taken from 1950 to 2005 (Figure 4c) show that
262 they started to increase in the mid 1950s, peaked in the late 1960s, and have decreased since
263 then. Locally, elevated atmospheric $\Delta^{14}\text{C}$ levels started to increase in 1995 for the west Enriched

264 Background Isotope Study site, but did not start to increase until 1999 for the east site. These
265 atmospheric $\Delta^{14}\text{C}$ values were assumed to be 0.0 before 1950. After 1995, the atmospheric Δ
266 ^{14}C values for the east and west sites were assumed to be equal to the observed yearly average of
267 new wood cellulose $\Delta^{14}\text{C}$ values.

268 The Enriched Background Isotope Study experiments were set up using four different model
269 runs where low and high $\Delta^{14}\text{C}$ labeled leaves were added to both the east and west sites. We
270 simulated the exclusion of ambient senescing leaves in the fall of 2000, 2001, and 2002 at all of
271 the sites, and then simulated their replacement by the addition of fixed masses of ambient and
272 high $\Delta^{14}\text{C}$ labeled leaves in May of 2001, and January of 2002 and 2003. The west site had
273 enriched $\Delta^{14}\text{C}$ roots and soil C because of the elevated atmospheric $\Delta^{14}\text{C}$ levels, while the east
274 site had background $\Delta^{14}\text{C}$ roots and soil C levels because of lower atmospheric $\Delta^{14}\text{C}$ levels
275 (Figure 4c).

276

277 **2.5. ForCent Model Calibration**

278 The data sets used to calibrate the parameters of the ForCent model include the observed
279 plant production data (by biomass pool) at the Oak Ridge National Laboratory from 1993 to
280 2000 [Hanson et al., 2003a], soil respiration data from 1993 to 2000 [Hanson et al., 2003b], and
281 the observed Enriched Background Isotope Study soil carbon $\Delta^{14}\text{C}$ data from 2000 to 2005 for
282 the surface litter, humus, and mineral soil layers (0-30 cm depth). We used a two-step process to
283 calibrate the ForCent model. The first step was to use the observed plant production and biomass
284 data from the Oak Ridge site to determine parameters in the plant production submodel. Most of
285 the plant production submodel parameters were estimated based on direct observations from this
286 site. The observed plant production and ecosystem carbon levels of the major plant parts

287 [*Hanson et al.*, 2003b] were used to determine the maximum live leaf area, turnover rates, and
288 allocation of carbon to the live fine root, branch, leaf, large wood, and coarse root pools. The
289 maximum maintenance respiration rates are 3.4 y^{-1} and 3.1 y^{-1} for juvenile and mature roots, and
290 were adjusted to match the total soil respiration rates observed at the Oak Ridge National
291 Laboratory site [*Hanson et al.*, 2003b]. The key assumption used for adjusting maintenance
292 respiration rates is that modeled heterotrophic respiration rates have greater certainty compared
293 to root maintenance respiration values. Maximum root death rates are 9.6 y^{-1} and 2.2 y^{-1} for
294 juvenile roots and mature roots are parameterized so that total fine root biomass matched the
295 *Joslin et al.* [2006] data set. This data set was also used to derive the fraction of carbon allocated
296 to root growth in the mineral soil and humus layers (95% and 5% respectively), the maximum
297 fraction of juvenile roots transferred to mature roots (1.5 y^{-1}), and the fraction of new root growth
298 allocated to juvenile roots (95%) and mature roots (5%). Growth respiration rate is assumed to be
299 23.3% for all of the live plant parts [*Hanson et al.*, 2003b]. The relative difference among the
300 maximum maintenance respiration rates for live leaves, fine branches, large wood, and coarse
301 roots was based on data from *Ryan et al.* [1996] showing that live leaves have the highest
302 respiration rates and that wood respiration rates are more than one order of magnitude lower than
303 live leaf respiration rates. Ecosystem nitrogen inputs were adjusted so that the observed mean
304 annual production matched the observed data.

305 The second step in the model calibration process was to use the observed time series (1972-
306 2004) of $\Delta^{14}\text{C}$ data for the mineral soil and humus layers to determine the mixing rate of humus
307 material into the mineral soil layer, the maximum decay rates for the humus layer, and the soil
308 mineral slow pool and passive soil organic matter pools. The model fitting process showed that
309 the site specific best fit to mineral soil $\Delta^{14}\text{C}$ was to have 40% of the mineral soil organic matter

310 in the slow pool for the west site and 55% for the east site. We used maximum turnover rates for
311 the slow and passive soil organic matter so that 47% of the total soil organic matter was slow
312 material in order to best fit the combined east and west mineral soil $\Delta^{14}\text{C}$ data. The maximum
313 turnover rate of the humus, mineral slow pools, and soil passive pools, and mixing of the humus
314 slow pool into the mineral soil layer, was estimated by finding parameters that resulted in the
315 best fit (minimum root mean square error) to the observed soil and litter layer $\Delta^{14}\text{C}$ data. There
316 is more uncertainty in these parameters since the observed soil $\Delta^{14}\text{C}$ data didn't include direct
317 measures of the turnover rates for the different soil organic matter pools.

318 Appendix 1 presents a list of the parameter values, including the definitions of the model
319 parameters which were adjusted to best fit observed data from the Oak Ridge site. Numerous
320 documents containing the information needed to reproduce the model results shown here, such as
321 the version of the ForCent model used in this paper, the computer code, user manuals, definitions
322 of all of the model parameters, guides on how to use the model, and weather data sets used to run
323 the model, can be downloaded from the following web site:

324 (<http://www.nrel.colostate.edu/projects/daycent/downloads.html>).

325

326 **3.0. Results**

327 **3.1. ForCent Model Verification**

328 From 1993 to 2000, model results compare favorably with observed mean plant production
329 (Table 1). Both the model and the data show that leaf production does not vary substantially
330 between years, while there are considerable year-to-year changes in fine root and wood plant
331 production. The absolute mean error of annual leaf and total plant production are less than 10%
332 of the mean annual production (6% and 9%), while absolute mean error for wood production and

333 fine root production are less than 20% of mean annual production (17% and 15%). Year-to-year
334 variability in live leaf, wood, and total production are reasonably well simulated with r^2 values
335 greater than 0.50 ($r^2 = 0.61, 0.60, \text{ and } 0.53$); however, yearly changes in fine root production are
336 not as well simulated with r^2 for fine roots less than 0.40. A comparison of the current ForCent
337 simulated annual plant production with results from earlier versions of the DayCent model show
338 that the ForCent model does a better job of simulating year-to-year changes in annual plant
339 production (earlier DayCent model had an $r^2 = 0.15$ and absolute mean error of $181 \text{ gm C m}^{-2} \text{ y}^{-1}$
340 for total plant production vs. $r^2 = 0.53$ and absolute mean error of 55.0 ForCent).

341 *Hanson et al.* [2003b] developed a data-based soil respiration model for predicting daily soil
342 respiration at the Oak Ridge National Laboratory site. The mean and range of the annual soil
343 respiration from 1993 to 2000 for the Hanson and ForCent models (Table 1) are quite similar, the
344 r^2 for the ForCent and Hanson model comparison for annual soil respiration is quite high ($r^2 =$
345 0.77), and the absolute mean error between the two models is less than 6% of the mean annual
346 soil respiration rate. A comparison of the Hanson and ForCent simulated daily soil respiration
347 results from the 1993 to 2000 shows that the results are quite similar for six years (r^2 range from
348 0.62 to 0.84), while during two of those years (1998 and 1999), the comparisons are less
349 favorable ($r^2 < 0.50$). Periods when the models do not agree occur when the ForCent model
350 simulates lower soil respiration rates because of lower than normal juvenile root biomass and
351 root production. Unfortunately, the limited observed daily soil respiration during those two years
352 doesn't allow us to determine which model is more accurate. A comparison of the ForCent
353 model predictions of daily soil respiration with the previous forest DayCent model
354 underestimated soil respiration on days with precipitation which resulted in a 50% to 100%
355 underestimate of soil respiration when observed respiration is $> 4 \text{ g C m}^{-2} \text{ d}^{-1}$.

356 Patterns for $\Delta^{14}\text{C}$ of the surface litter, humus, and the 0-30 cm mineral layers for the
357 enriched and near-background litter addition treatments (Figures 5 and 6; Table 2) show a
358 general agreement between the model results and observed data. The model and data show that
359 the $\Delta^{14}\text{C}$ content of the surface litter layer (Figure 5) is higher for the west site compared to the
360 east site, and that the near-background litter treatment has lower $\Delta^{14}\text{C}$ content compared to the
361 enriched treatment. The overall fit of the model to the observed data is similar for both the east
362 and west sites, and the mean absolute error (Table 2) ranges from 27 gm C m^{-2} for the east site
363 low treatment to 52 gm C m^{-2} for the west site low treatment. The higher surface litter $\Delta^{14}\text{C}$
364 content of the west site compared to the east site reflects the higher atmospheric $\Delta^{14}\text{C}$ content of
365 the west site (Figure 4a).

366 A comparison of observed and simulated $\Delta^{14}\text{C}$ of the humus layer (Figure 5c,d) shows
367 increased $\Delta^{14}\text{C}$ levels for enriched litter additions. The ForCent simulations for the west site
368 capture the $\Delta^{14}\text{C}$ increase of the humus layer beginning in 1999, following the large atmospheric
369 $\Delta^{14}\text{C}$ exposures (see Figure 4a). This contrasts with the simulated humus $\Delta^{14}\text{C}$ levels in the east
370 site which decrease until 2000, and then stabilize around 190‰ for ambient plots with near-
371 background litter additions. The model results compare well, yet the results from the east site are
372 more consistent with fewer discrepancies. The absolute mean errors are much lower for the high
373 and low treatments for the east site (21 and 8 gm C m^{-2}) compared to the west site (53 and 85 gm
374 C m^{-2}). This pattern of better fit of the model to observed data from the east site is true for both
375 the humus layer and the surface litter layer. The major discrepancy for the humus layer is an
376 underestimate of the west site $\Delta^{14}\text{C}$ value for 2001. It was impossible to adjust the maximum
377 turnover rate of the humus layer to fit both the 2001 point and the observations from 2002 to
378 2005.

379 A comparison of the observed and simulated soil mineral $\Delta^{14}\text{C}$ (0-30 cm soil depth) values
380 from 1950 to 2005 (Figure 6a) for the low east site shows that the soil $\Delta^{14}\text{C}$ values peaked from
381 1975 to 1985, and then started to decrease. The major discrepancy is the model underestimate of
382 the soil $\Delta^{14}\text{C}$ in 1973 which is likely a result from the fact that the observed 1973 $\Delta^{14}\text{C}$ value is
383 for the 0-15 cm depth (simulated 0-30 cm depth soil includes older soil that has not been
384 impacted by the recent increases in atmospheric $\Delta^{14}\text{C}$ bomb carbon). Model results for the east
385 site show a continuing pattern of decreasing $\Delta^{14}\text{C}$ values for both litter addition treatments from
386 1995 to 2005 (Figure 6b). This contrasts with the west site results after 1999 where increases in
387 soil $\Delta^{14}\text{C}$ are observed and simulated (Figure 6b). The observed data is consistent with
388 simulations showing higher soil $\Delta^{14}\text{C}$ values for the west site compared to the east site, and
389 higher values of $\Delta^{14}\text{C}$ by 2005 for the enriched litter treatment. The observed vs. simulated mean
390 absolute error for the mineral soil $\Delta^{14}\text{C}$ values in the high and low treatments in the west site is
391 lower (10 and 8 gm C m^{-2}) compared to the east site (12 and 14 gm C m^{-2}). The biggest model
392 discrepancy is an underestimate of the east site low treatment humus $\Delta^{14}\text{C}$. The standard
393 deviation for the observed mineral soil $\Delta^{14}\text{C}$ data is quite high for both sites.

394

395 **3.2. Model Validation Comparisons**

396 The Enriched Background Isotope Study soil respiration $\Delta^{14}\text{C}$ data for the mineral soil,
397 humus, and surface litter layers, and for total soil respiration, along with the dead and live root Δ
398 ^{14}C data, were not used in the model calibration process, and as a result, could be used to validate
399 model predictions. A comparison of the observed vs. simulated $\Delta^{14}\text{C}$ values for the live and
400 dead roots for the east and west sites (Figure 7) generally agree with higher $\Delta^{14}\text{C}$ values for the
401 dead and live roots in the west site, and a pattern of decreasing $\Delta^{14}\text{C}$ values from 1999 until

402 2004 for both sites. The elevated $\Delta^{14}\text{C}$ values after 2004 are due to increased atmospheric $\Delta^{14}\text{C}$
403 for both the east and west sites (higher increases in the west site). A comparison of the simulated
404 live juvenile root $\Delta^{14}\text{C}$ values with the new root growth screen data (Figure 7c - root biomass
405 that grows in screens inserted into the soil) shows that the model correctly predicts the observed
406 decreases in $\Delta^{14}\text{C}$ values following the 1999 atmospheric labeling events; higher $\Delta^{14}\text{C}$ values
407 for the west site compared to the east site, and the observed increase in $\Delta^{14}\text{C}$ values in 2004 and
408 2005. The major discrepancy is an overestimate of live (total root biomass and juvenile roots)
409 and dead root $\Delta^{14}\text{C}$ values by the model for the west site from 2001 to 2004.

410 Simulated total soil respiration and $\Delta^{14}\text{C}$ values for the west site during August 2003 (Figure
411 8) show large day-to-day changes in total soil respiration and spikes in the $\Delta^{14}\text{C}$ values for the
412 high ^{14}C litter treatments associated with rainfall events. These results are consistent with the
413 data from *Cisneros-Dozal et al.* [2007] showing a 50-100% increase in soil respiration $\Delta^{14}\text{C}$
414 values following rainfall events for the high treatments and minimal changes in $\Delta^{14}\text{C}$ of soil
415 respiration following rainfall events for the low treatments. Increases in the $\Delta^{14}\text{C}$ of soil
416 respiration following rainfall events for the high treatments are caused by rainfall-induced
417 increased decomposition of the highly labeled surface litter layer (surface litter and humus
418 layers).

419 A comparison of the observed vs. simulated $\Delta^{14}\text{C}$ soil respiration values for all of the soil
420 pools and different treatments (Figure 9) shows that the model performed well, representing the
421 observed data set ($r^2 = 0.75$). Simulated mean mineral soil respiration $\Delta^{14}\text{C}$ values (Figure 9a)
422 follow a pattern of higher $\Delta^{14}\text{C}$ levels in the east site; however, the model tends to underestimate
423 the observed increase in $\Delta^{14}\text{C}$ levels for the high vs. low treatments at both the east and west
424 sites. Our results suggest that the model underestimated the amount of labeled aboveground litter

425 dissolved organic carbon transported to the mineral soil layer, and lost as soil respiration from
426 the mineral soil layer. Simulated and observed 2001 soil respiration $\Delta^{14}\text{C}$ values for the surface
427 litter and humus layers (Figure 9b) follow the general pattern of higher values for the west site,
428 and an increase in $\Delta^{14}\text{C}$ levels with the high treatment. The model tends to underestimate the
429 humus layer $\Delta^{14}\text{C}$ content and also appears to be underestimating the amount of the elevated Δ
430 ^{14}C material that is transferred to the humus layer for the west site.

431

432 **3.3. Sensitivity Analysis**

433 The model tuning process revealed that results are sensitive to the assumed values of the
434 atmospheric $\Delta^{14}\text{C}$ values on the east and west sites, and also to the fraction of the mineral soil
435 organic matter in the passive pool (Figure 1). We assumed that the atmospheric $\Delta^{14}\text{C}$ values for
436 the east and west sites were equal to the observed $\Delta^{14}\text{C}$ values of new wood cellulose. Observed
437 atmospheric $\Delta^{14}\text{C}$ values for the east and west sites were measured from 2001 to 2005, showing
438 variability both within the year and among different years. The impact of changing the
439 atmospheric $\Delta^{14}\text{C}$ values by $\pm 30\%$ after 1995 on simulated mineral soil $\Delta^{14}\text{C}$ values (Figure
440 10a,b) shows that the model best fit the west site observed soil $\Delta^{14}\text{C}$ values for the high and low
441 treatments with a 30% increase in atmospheric $\Delta^{14}\text{C}$ levels. Similar results are also found for the
442 simulated $\Delta^{14}\text{C}$ values for the humus layer (data not presented) in the high and low treatment
443 model runs for the west site, thus suggesting that the mean atmospheric $\Delta^{14}\text{C}$ values were
444 underestimated by the cellulose $\Delta^{14}\text{C}$ values in the west site. Unfortunately, model results for the
445 simulated live and dead roots in the east site don't agree with these results since elevating the
446 atmospheric $\Delta^{14}\text{C}$ values by 30% increased the simulated overestimate of the live and dead root

447 $\Delta^{14}\text{C}$ values (data not shown). Results for the east site (Figure 10c,d) show that the best model
448 results for the mineral soil $\Delta^{14}\text{C}$ values occur with a 30% reduction in atmospheric $\Delta^{14}\text{C}$ values.

449 The best fit estimate of the fraction of mineral soil organic matter in the passive fraction for
450 combined east and west sites was 47%. We kept the total mineral soil organic matter fixed and
451 altered the decay rates of slow and passive pools in order to set up computer model runs with
452 40% and 55% passive soil organic matter. Results for the east site (Figure 11a,b) showed that the
453 best fit to the observed mineral soil $\Delta^{14}\text{C}$ data was obtained with 55% passive soil organic
454 matter. The improved fit to the observed data was clearest for the east site low treatment where
455 the model overestimated the observed soil $\Delta^{14}\text{C}$ values. Opposite results were observed for the
456 west site where the 40% passive run was best fit to the observed high and low mineral soil $\Delta^{14}\text{C}$
457 values.

458

459 **4. Discussion**

460 We demonstrate here that the ForCent model can successfully simulate carbon dynamics of
461 deciduous forest systems. Model results were compared with observed plant production data,
462 carbon in the soil and plant pools, and $\Delta^{14}\text{C}$ dynamics for plants and soils during the Enriched
463 Background Isotope Study experiment. Data from the Oak Ridge National Laboratory site was
464 used to make major changes to the ForCent model and calibrate some of the parameters. The
465 major improvements in the model include adding a detailed root growth model, a dynamic plant
466 carbon allocation scheme, a surface humus layer, plant phenology in the plant production
467 submodel, including a rainfall pulse response to the surface litter decay, and adding a plant
468 stored carbohydrate pool. A comparison of the earlier DayCent model results show that the new
469 ForCent model greatly improved the ability of the model to simulate year to year changes in

470 forest plant production (total plant production r^2 increased from 0.19 to 0.52). The process of
471 adding plant phenology and seasonal patterns in wood growth (wood growth ceases at the end of
472 July) resulted in a decrease in the simulated inter-annual variability of plant production,
473 consistent with the observed inter-annual production data [Hanson et al., 2003a]. Stopping wood
474 growth at the end of July results in plant storage of soil nutrients from August to October, and
475 then utilized during the next growing season.

476 One of the major improvements in the ForCent model was to include the precipitation pulse
477 event multiplier for the surface litter decay based on the Hanson et al. [2003a] data-based soil
478 respiration model. Comparison of the Hanson- and ForCent-simulated daily soil respiration rates,
479 taken from 1993 to 2000 for the Oak Ridge National Laboratory site, showed close agreement
480 with the observed data for both models ($r^2 = 0.61$ and 0.64). Comparison of the daily simulated
481 soil respiration for the Hanson and ForCent models for six of the eight years was quite good (r^2
482 ranging from 0.72 to 0.84). The ForCent model predicted lower soil respiration compared to the
483 Hanson model during two of the years when ForCent predicted lower than average live root
484 biomass and root production. Lower total soil respiration simulated by ForCent during these time
485 periods resulted from reduced autotrophic respiration (maintenance plus growth) from the live
486 roots. Root dynamics in the ForCent model are quite dynamic and respond to year-to-year
487 differences in plant production and water stress, while the Hanson model assumed root growth
488 patterns were less dynamic. It is not clear which model is correct since we did not have sufficient
489 observed data during the time periods when the major ForCent and Hanson model differences
490 were observed.

491 The ForCent model correctly simulated higher $\Delta^{14}\text{C}$ levels for the surface litter and mineral
492 soil pools in the west site, higher $\Delta^{14}\text{C}$ levels for the high labeled litter treatment, and also the

493 incorporation of highly labeled leaf litter into the humus layer. Simulated results for the west site
494 showed lower $\Delta^{14}\text{C}$ levels for mineral soil and humus layers compared to the observed data and
495 suggest that the atmospheric $\Delta^{14}\text{C}$ levels for the west site might be underestimated. A sensitivity
496 analysis suggests that increasing the assumed atmospheric $\Delta^{14}\text{C}$ levels from 1995 to 2005 results
497 in an improved fit of the model results for the mineral soil and humus layer $\Delta^{14}\text{C}$ levels for the
498 west site. The results from the observed and simulated west site root $\Delta^{14}\text{C}$ data suggest that west
499 site atmospheric $\Delta^{14}\text{C}$ should be decreased and thus are inconsistent with mineral soil $\Delta^{14}\text{C}$
500 data. Results from the east site show that decreasing the atmospheric $\Delta^{14}\text{C}$ level results in a
501 better fit to the observed mineral soil $\Delta^{14}\text{C}$ levels.

502 The model fitting process and sensitivity analysis revealed that it is possible to correctly
503 simulate the observed temporal changes in the mineral soil $\Delta^{14}\text{C}$ values during the last 50 years
504 using different assumptions about the fraction of the total mineral soil carbon in the passive soil
505 organic matter pool (40-55%). We chose to fit the model using 47% since the best fit for the
506 passive fractionation for the west site was 55% and was 40% for the east site. The new estimates
507 of the turnover rates for slow and passive soil organic matter are different from the original
508 Century model estimates [*Parton et al.*, 1987], with the decay rate for passive soil organic matter
509 decreased by 50% and the slow decay rate increased by 100% compared to the original values.
510 *Falloon et al.* [1998] fit the RothC model to a similar data set at the Rothamsted site in England
511 and assumed that the passive fraction (inert fraction in RothC) was only 10% of the soil organic
512 matter pool. *Petersen et al.* [2005a, 2005b] used the CN-SIM model to simulate the changes in
513 the mineral soil $\Delta^{14}\text{C}$ values during the last 50 years at three sites in Europe, and found that
514 equally good fits to the observed data were between 10% and 50% of mineral soil organic matter
515 in the inert fraction. A comparison of the results from the RothC, CN-SIM, and ForCent models

516 shows that the peak mineral soil $\Delta^{14}\text{C}$ values occurred from 1975 to 1985 and had a similar
517 temporal pattern during the last 50 years (increasing after 1957 and then decreasing after 1985).
518 The results from the three different models show that there is considerable uncertainty in our
519 estimates of the fraction of total mineral soil C in passive soil organic matter and in the decay
520 rates of the slow and passive (or inert) pools.

521 Observed differences between the high and low treatment mineral soil $\Delta^{14}\text{C}$ values show a
522 slight increase for the high treatments. This increase is difficult to measure because of the large
523 amount of carbon in the 0-15 cm soil layer, and suggests that our estimate of the mixing rate of
524 humus material into the mineral soil layer is not well bounded. We are starting a new multi-site
525 ^{14}C surface litter layer experiment which will allow us to better quantify this flux since we will
526 be measuring the 0-5 cm mineral soil layer instead of the 0-15 cm layer used in the Enriched
527 Background Isotope Study experiment. Future re-sampling of the of the $\Delta^{14}\text{C}$ values of the
528 humus and mineral soil layers from the Enriched Background Isotope Study experimental plots
529 will also provide data to better quantify the mixing rate of humus material into the mineral soil.

530 We used the observed Enriched Background Isotope Study $\Delta^{14}\text{C}$ data for live and dead fine
531 root and soil respiration, surface litter, and layers to validate ForCent simulations (data not used
532 for model calibration) of the movement of ^{14}C into the soil pools. ForCent correctly simulated
533 the observed higher $\Delta^{14}\text{C}$ values for live and dead roots in the west site and also the general
534 pattern of decreasing $\Delta^{14}\text{C}$ values following the 1999 exposure to elevated ^{14}C atmospheric
535 levels. However, the model did tend to overestimate the $\Delta^{14}\text{C}$ values for live roots in the west
536 site. The sensitivity analysis showed that increasing the atmospheric $\Delta^{14}\text{C}$ values in the west site
537 improved the fit of the model to the humus and mineral soil $\Delta^{14}\text{C}$ values. This increase caused

538 the model to exaggerate the existing overestimate of the live and dead root $\Delta^{14}\text{C}$ values for the
539 west site.

540 A comparison of the observed vs. simulated soil respiration $\Delta^{14}\text{C}$ values shows that the
541 model correctly simulated the major Enriched Background Isotope Study treatment differences
542 and the movement of $\Delta^{14}\text{C}$ labeled leaf and root carbon into soil organic matter pools (observed
543 vs. simulated $r^2 = 0.75$ overall). The model tended to underestimate the observed increase in
544 mineral soil respiration $\Delta^{14}\text{C}$ values for the high labeled litter treatments. This could result from
545 an underestimate of the amount of labile surface litter material leaching out of the surface litter
546 layer into the mineral soil layer and then quickly lost due to microbial respiration. Dissolved
547 organic carbon flux measurements for the Enriched Background Isotope Study experiment
548 [Fröberg *et al.*, 2007; Fröberg *et al.*, 2009] show that a substantial amount of dissolved organic
549 carbon is leached out of the surface litter layer (surface litter, humus layers) into the mineral soil
550 layer and quickly lost as soil respiration. These data from Fröberg *et al.* [2009] are currently
551 being used to develop a new dissolved organic carbon leaching submodel in ForCent.

552

553 **Acknowledgements**

554 Funding for the Enriched Background Isotope Study project was provided by the U.S.
555 Department of Energy, Office of Science, Office of Biological and Environmental Research
556 under Contract No. DE-AC02-05CH11231, as a part of the Terrestrial Carbon Processes (TCP)
557 Program.

558

559

560

561 **References**

- 562 Aerts, R., H. de Caluwe, and B. Beltman, (2003), Plant community mediated vs. nutritional
563 controls on litter decomposition rates in grasslands, *Ecology*, 84(12), 3198-3208.
- 564 Cisneros-Dozal, L. M., S. E. Trumbore, and P. J. Hanson, (2007), Effect of moisture on leaf litter
565 decomposition and its contribution to soil respiration in a temperate forest, *J. Geophys.*
566 *Res.*, 112, G01013, doi:10.1029/2006JG000197.
- 567 Coleman, K., and D. S. Jenkinson (1996), RothC-26.3 — A model for the turnover of carbon in
568 soil, in *Evaluation of soil organic matter models using existing long-term datasets*, vol.
569 38, edited by S. Powelson, P. Smith, and J. U. Smith, pp. 237-246, Springer, Berlin
- 570 DelGrosso, S. J., A. R. Mosier, and W. J. Parton (2005), DAYCENT model analysis of past and
571 contemporary soil N₂O and net greenhouse gas flux for major crops in the USA, *Soil and*
572 *Tillage Research*, 83, 9-24.
- 573 DelGrosso, S. J., W. J. Parton, and A. R. Mosier (2001a), Simulated interaction of carbon
574 dynamics and nitrogen trace gas fluxes using the DAYCENT model, in *Modeling Carbon*
575 *and Nitrogen Dynamics for Soil Management*, edited by M. Schaffer, L. Ma, and S.
576 Hansen, CRC Press, Boca Raton, Florida.
- 577 DelGrosso, S. J., W. J. Parton, and A. R. Mosier (2001b), Simulated effects of land use, soil
578 texture, and precipitation on N gas emissions using DAYCENT, in *Nitrogen in the*
579 *Environment: Sources, Problems, and Management*, edited by R. F. Follett, and J. L.
580 Hatfield, Elsevier Science Publishers, The Netherlands.
- 581 DeLucia, E. H., J. E. Drake, R. B. Thomas, M. Gonzalez-Meier (2007), Forest carbon use
582 efficiency: is respiration a constant fraction of gross primary production? *Global Change*
583 *Biology*, 13, 1157-1167.

- 584 Dornbush, M. E., T. M. Isenhardt, J. W. Raich (2002), Quantifying fine-root decomposition: An
585 alternative to buried litterbags, *Ecology*, 83, 2985-2990.
- 586 Eitzinger, J., W. J. Parton, and M. Hartman (2000), Improvement and validation of a daily soil
587 temperature submodel for freezing/thawing periods, *Soil Sci.*, 165(7), 525-534.
- 588 Follett, R. F., E. A. Paul, and E. G. Pruessner (2007), Soil carbon dynamics during a long-term
589 incubation study involving ^{13}C and ^{14}C measurements, *Soil Biol. Biochem.*, 172, 189-208.
- 590 Falloon, P. D., P. Smith, and K. Coleman (1998), Estimating the size of the inert organic matter
591 pool for use in the Rothamsted carbon model, *Soil Biol. Biochem.*, 28, 1367-1372.
- 592 Fröberg, M., P. J. Hanson, S. E. Trumbore, C. W. Swanston, and D. E. Todd (2009), Flux of
593 carbon from ^{14}C -enriched leaf litter throughout a forest soil mesocosm, *Geoderma*, 149,
594 181-188.
- 595 Fröberg, M., P. M. Jardine, and P. J. Hanson (2007), Low dissolved organic carbon input from
596 fresh litter to deep mineral soils. *Soil Sci. Soc. Am. J.*, 71, 347-354.
- 597 Frohking, S. E., A. R. Mosier, and D. S. Ojima (1998), Comparison of N_2O emissions from soils
598 at three temperate agricultural sites: simulations of year-round measurements by four
599 models, *Nutrient Cycling in Agroecosystems*, 52, 77-105.
- 600 Hanson, P. J., C. W. Swanston, and C. T. Gartner Jr. (2005), Reconciling change in Oi-horizon
601 carbon-14 with mass loss for an oak forest, *Soil Sci. Soc. Am. J.*, 69, 1492-1502.
- 602 Hanson, P. J., D. E. Todd, and D. C. West (2003a), Tree and sapling growth and mortality, in
603 *North American Temperate Deciduous Forest Responses to Changing Precipitation*
604 *Regimes*, edited by P. J. Hanson, and S. D. Wullschleger, Springer, New York.
- 605 Hanson, P. J., E. G. O'Neill, and M. L. S. Chambers (2003b), Soil respiration and litter
606 decomposition, in *North American Temperate Deciduous Forest Responses to Changing*

- 607 *Precipitation Regimes*, edited by P. J. Hanson, and S. D. Wullschleger, Springer, New
608 York.
- 609 Hobbie, S. E. (1996), Temperature and plant species control over litter decomposition in Alaskan
610 tundra. *Ecological Monographs*, 66, 503-522.
- 611 Jenkinson, D. S. (1971) Studies on the decomposition of ¹⁴C-labeled organic matter in soil, *Soil*
612 *Sci.*, 111, 64-70.
- 613 Joslin, J. D., J. B. Gaudinski, and M. S. Torn (2006), Fine root turnover patterns and their
614 relationship to root diameter and soil depth in a ¹⁴C-labeled hardwood forest, *New*
615 *Phytologist*, 172, 523-535.
- 616 Kelly, R. H., W. J. Parton, and M. D. Hartman (2000), Intra- and inter-annual variability of
617 ecosystem processes in shortgrass steppe, *J. Geophys. Res.: Atmospheres*, 105, 20,093-
618 20,100.
- 619 Kelly, R. H., W. J. Parton, and C. J. Crocker (1997), Simulating trends in soil organic carbon in
620 long-term experiments using the Century model, *Geoderma*, 81, 75-90.
- 621 Li, C., S. Frolking, and R. Harriss, (1994), Modeling Carbon Biogeochemistry in Agricultural
622 Soils, *Global Biogeochem. Cycles* 8(3), 237-254.
- 623 Litton, C. M., M. G. Ryan, J. W. Raich (2007), Carbon allocation in forest ecosystems, *Global*
624 *Change Biology*, 13, 2089-2109.
- 625 Lousier, J. D., and D. Parkinson (1976), Litter decomposition in a cool temperature deciduous
626 forest, *Can. J. Botany*, 54, 419-436.
- 627 Luo, Y., D. Gerten, G. Le Marie, W. J. Parton, E. Weng, X. Zhou, C. Keough, C. Beier, P. Ciais,
628 W. Cramer, J. S. Dukes, B. Emmett, P. J. Hanson, A. Knapp, S. Linder, D. Nepstad, and
629 L. Rustad (2008), Modeled interactive effects of precipitation, temperature, and CO₂ on

- 630 ecosystem carbon and water dynamics in different climatic zones, *Global Change*
631 *Biology*, 14, 1986-1999.
- 632 McClaran, M. P., and G. R. McPherson (1995), Can soil organic carbon isotopes be used to
633 describe grass-tree dynamics at a savanna-grassland ecotone and within the savanna? *J.*
634 *Vegetation Science*, 6(6), 857-862.
- 635 McClaugherty, C. A., J. Pastor, and J. D. Aber (1985), Forest litter decomposition in relation to
636 soil nitrogen dynamics and litter quality, *Ecology*, 66(1), 266-275.
- 637 Meentemeyer, V. (1978), Macroclimate the lignin control of litter decomposition rates, *Ecology*,
638 59(3), 465-472.
- 639 Melillo, J. M., J. D. Aber, and J. F. Muratore (1982), Nitrogen and lignin control of hardwood
640 leaf litter decomposition dynamics, *Ecology*, 63(3), 621-626.
- 641 Osher, L. J., P. A. Matson, and R. Amundson (2003), Effect of land use change on soil carbon in
642 Hawaii, *Biogeochemistry*, 65(2), 213-232.
- 643 Parton, W. J., W. L. Silver, and I. C. Burke (2007a), Global-scale similarities in nitrogen release
644 patterns during long-term decomposition, *Science*, 315, 361-164.
- 645 Parton, W. J., J. A. Morgan, G. Wang (2007b), Projected ecosystem impact of the prairie heating
646 and CO₂ enrichment experiment, *New Phytologist*, 174, 823-834.
- 647 Parton, W. J., E. A. Holland, and S. J. Del Grosso (2001), Generalized model for NO_x and N₂O
648 emissions from soils, *J. Geophys. Res.*, 106, 17403-17420.
- 649 Parton, W. J., M. Hartman, and D. S. Ojima (1998), DAYCENT and its land surface submodel:
650 description and testing, *Global and Planetary Change*, 19, 35-48.
- 651 Parton, W. J., D. S. Schimel, and C. V. Cole (1987), Analysis of factors controlling SOM levels
652 in Great Plains grasslands, *Soil Sci. Soc. Am. J.*, 51, 1173-1179.

- 653 Parton, W. J., J. S. Singh, and D. C. Coleman (1978) A model of production and turnover of
654 roots in shortgrass prairie, *J. Appl. Ecology*, 47, 515-542.
- 655 Paul, E. A., R. F. Follett, and S. W. Leavitt (1997), Radiocarbon dating for determination of
656 SOM pool sizes and dynamics, *Soil Sci. Soc. Am. J.*, 61, 1058-1067.
- 657 Pepper, D. A., S. J. DelGrosso, and R. E. McMurtrie (2005) Simulated carbon sink response of
658 shortgrass steppe, tallgrass prairie, and forest ecosystems to rising (CO₂) temperature and
659 nitrogen input, *Global Biogeochem. Cycles*, 19, GB1004, doi:10.1029/2004GB002226.
- 660 Petersen, B. M., J. Berntsen, and S. Hansen (2005a), CN-SIM - a model for the turnover of
661 SOM. I: Long term carbon development, *Soil Biol. Biochem.*, 37, 359-374.
- 662 Petersen, B. M., L. S. Jensen, J. Berntsen, and S. Hansen (2005b), CN-SIM - a model for the
663 turnover of SOM. II: Short term carbon and nitrogen development, *Soil Biol. Biochem.*,
664 37, 375-393.
- 665 Riley, W. J., J. B. Gaudinski, M. S. Torn, J. D. Joslin, and P. J. Hanson (2009), Fine-root
666 mortality rates in a temperate forest: estimates using radiocarbon data and numerical
667 modeling, *New Phytologist*, 184, 387-398.
- 668 Running, S. W., and J. C. Coughlan (1988), A general model of forest ecosystem processes for
669 regional applications, I. Hydrologic balance, canopy gas exchange and primary
670 production processes, *Ecological Modelling*, 42, 125-154.
- 671 Ryan, M. G., R. M. Hubbard, S. Pongracic, R. J. Raison, R. E. McMurtrie (1996), Foliage, fine-
672 root, woody-tissue and stand respiration in *Pinus radiata* in relation to nitrogen status,
673 *Tree Physiology*, 16, 333-343.
- 674 Ryan, M. G., S. T. Gower, and R. M. Hubbard (1995), Woody tissue maintenance respiration of
675 four conifers in contrasting climates, *Oecologia*, 101, 133-140.

- 676 Shanks, R. E., and J. S. Olson (1961) First-year breakdown of leaf litter in southern Appalachian
677 forests, *Science*, 134, 194-195.
- 678 Steuter, A. A., B. Jasch, and J. Ihnen (1990) Woodland/grassland boundary changes in the
679 middle Niobrara Valley of Nebraska identified by $\delta^{13}\text{C}$ values of SOM, *American*
680 *Midland Naturalist*, 124(2), 301-308.
- 681 Swanston, C. W., M. S. Torn, and P. J. Hanson (2005), Initial characterization of processes of
682 soil carbon stabilization using forest stand-level radiocarbon enrichment, *Geoderma*, 128,
683 52-62.
- 684 Trofymow, J. A., T. R. Moore, and B. D. Titus (2002), Rates of litter decomposition over 6 years
685 in Canadian forests: influence of litter quality and climate, *Can. J. Forest Research*, 32,
686 789-804.
- 687 Trumbore, S., J. B. Gaudinski, and P. J. Hanson (2002), A whole-ecosystem carbon-14 label in a
688 temperate forest, *EOS*, 83(265), 267-268.
- 689 Wang, Y, R. Amundson, and S. Trumbore (1996), Radiocarbon dating of SOM, *Quaternary*
690 *Research*, 45(3), 282-288.
- 691 Waring, R. H., J. J. Landsberg, M. Williams (1998), Net primary production of forests: a
692 constant fraction of gross primary production? *Tree Physiology*, 18, 129-134.
- 693 Wieder, R. K., G. E. Lang (1982), A critique of the analytical methods used in examining
694 decomposition data obtained from litter bags, *Ecology*, 63(6), 1636-1642.

Table 1. Comparison of observed and simulated plant production for leaves, fine roots, total wood production, total production, and soil respiration from 1993-2000 at the Oak Ridge site [Hanson *et al.*, 2003a, 2003b]. The table also contains the maximum and minimum annual flux values during the time period, the mean absolute error and r^2 values for the model vs. observed data comparison.

Annual Plant Production	Simulated mean (g C/m² y⁻¹)	Observed mean (g C/m² y⁻¹)	Mean absolute error* (g C m⁻² y⁻¹)	Model vs. observed data (r²)
Leaf	246.0 (230 – 249)	240.0 (233 – 258)	14.0	0.61
Wood (branch + Large wood + Coarse roots)	267.0 (99 – 374)	264.0 (200 – 348)	43.0	0.60
Fine roots	116.0 (67 – 136)	113.0 (89 – 153)	17.0	0.38
Total production	629.0 (413 – 753)	616.0 (529 – 747)	55.0	0.53
Soil respiration	916.0 (809 – 1024)	941.0 (808 – 976)	52.0	0.77**

* Mean absolute error $\frac{\sum_{t=1}^N \text{abs}(S_i - O_i)}{N}$ where O_i is the observed value, S_i is the simulated value and N is the number of observations.

** Data from 1998 and 1999 were excluded because of uncertainty about which model was correct (see discussion in text)

Table 2: Comparison of the observed and simulated mean $\Delta^{14}\text{C}$ for surface litter, humus, and mineral soil for the east and west sites and high and low treatments. The mean absolute error for the surface litter, humus, and mineral soil layer is also presented.

		Observed Mean	Simulated Mean	Mean Absolute
		$\Delta^{14}\text{C}$ (‰)	$\Delta^{14}\text{C}$ (‰)	Error*
Surface Litter				
East	High	503.0	478.0	52.0
	Low	211.0	211.0	27.0
West	High	646.0	628.0	42.0
	Low	358.0	361.0	48.0
Humus				
East	High	266.0	200.0	21.0
	Low	200.0	201.0	8.0
West	High	405.0	351.0	53.0
	Low	357.0	272.0	85.0
Carbon				
Soil East	High	119.0	125.0	12.0
	Low	108.0	122.0	14.0
Soil West	High	146.0	142.0	10.0
	Low	143.0	139.0	8.0

*Mean absolute error = $\frac{\sum_{i=1}^N \text{abs}(O_i - S_i)}{N}$ where O_i is the observed value, S_i is the simulated value, and N is the number of observations.

1 **Figure Captions**

2 Figure 1. Flow diagram and components of the ForCent forest growth model. The ForCent
3 model simulates $\Delta^{14}\text{C}$ and $\Delta^{13}\text{C}$ content for all of the carbon state variables and flows in the
4 model (e.g., soil respiration).

5 Figure 2. Revised flow diagram for the surface organic and mineral soil layers in the ForCent
6 model.

7 Figure 3. Fine root growth submodel used in the ForCent model. This model is based on the
8 model developed by *Parton et al.* [1978].

9 Figure 4. (a) Impact of soil relative water content [F (W)] on decomposition of ForCent soil
10 pools; (b) the effect of soil temperature [F (T)] on the decomposition of soil pools; and (c)
11 observed atmospheric $\Delta^{14}\text{C}$ levels from 1950 to 2005 for the east and west EBIS experimental
12 sites. Atmospheric $\Delta^{14}\text{C}$ values for the east and west sites from 1995 to 2006 are based on
13 observed average wood cellulose values for these sites.

14 Figure 5. Simulated vs. observed $\Delta^{14}\text{C}$ content of the surface litter layer for the (a) east, and (b)
15 west sites. Simulated vs. observed $\Delta^{14}\text{C}$ content of the humus layer for the (c) east, and (d) west
16 EBIS sites. Data is presented for both the low and high litter treatments in addition to the
17 standard deviation of the observed data.

18 Figure 6. Simulated vs. observed mineral soil layer $\Delta^{14}\text{C}$ content for the (a) low east site from
19 1950 to 2005; (b) low and high east site mineral soil $\Delta^{14}\text{C}$ values from 1995 to 2005; and (c)
20 west site (high and low treatments) mineral soil $\Delta^{14}\text{C}$ values from 1995 to 2005. Data from the Δ

21 ^{14}C levels prior to 2001 came from the Walker branch site, and standard deviation of the
22 observed data is plotted.

23 Figure 7. Simulated vs. observed $\Delta^{14}\text{C}$ levels for the (a) dead roots in the east and west sites; (b)
24 live roots in the east and west sites; and (c) a comparison of simulated $\Delta^{14}\text{C}$ values for live
25 juvenile roots with the observed root screen new root growth $\Delta^{14}\text{C}$ data for the east and west
26 sites (plus the standard deviation of the observed data).

27 Figure 8. (a) Simulated total soil respiration from August 2003 in response to rainfall events; and
28 (b) observed vs. simulated $\Delta^{14}\text{C}$ of total soil respiration for the high and low treatments at the
29 east site [Cisneros-Dozal *et al.*, 2007].

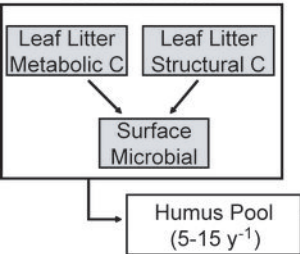
30 Figure 9. Comparison of observed and simulated average $\Delta^{14}\text{C}$ values for total soil respiration,
31 litter respiration (surface litter plus humus layers), and mineral soil respiration from 2002 to
32 2004 for (a) east and west site high and low treatments; and (b) average humus and surface litter
33 $\Delta^{14}\text{C}$ respiration from the east and west site high and low treatments for 2001.

34 Figure 10. Comparison of observed and simulated mineral soil $\Delta^{14}\text{C}$ values for the control runs,
35 and $\pm 30\%$ atmospheric $\Delta^{14}\text{C}$ runs for (a) the east high treatment; (b) east low treatment; (c) west
36 high treatment; and (d) west low treatment. Control atmospheric $\Delta^{14}\text{C}$ values for the east and
37 west sites from 1995 to 2006 were assumed to be equal to the average new cellulose wood
38 growth $\Delta^{14}\text{C}$ values in the east and west sites.

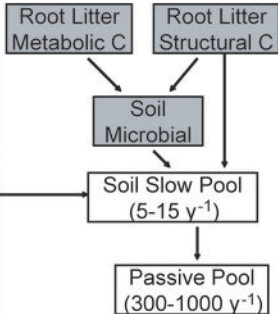
39 Figure 11. Comparison of the observed and simulated mineral soil $\Delta^{14}\text{C}$ values for the 47%
40 passive SOM pool run, 40% passive SOM pool run, and 57% passive SOM pool run for the (a)
41 east high treatment; (b) east low treatment; (c) west high treatment; and (d) west low treatment.

EBIS *ForCent* C Pools

Surface Litter

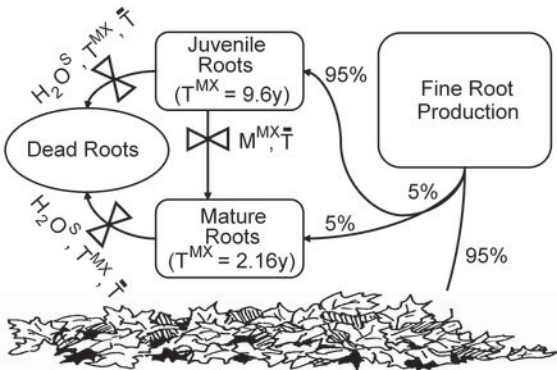


Mineral Soil (0-30cm)

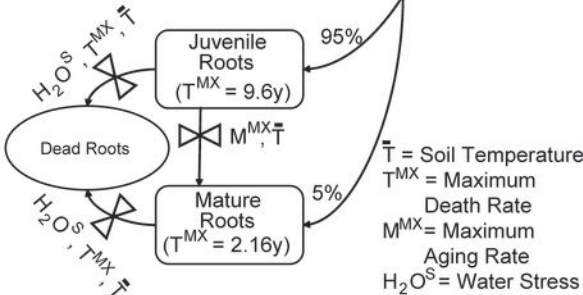


Fine Root Model

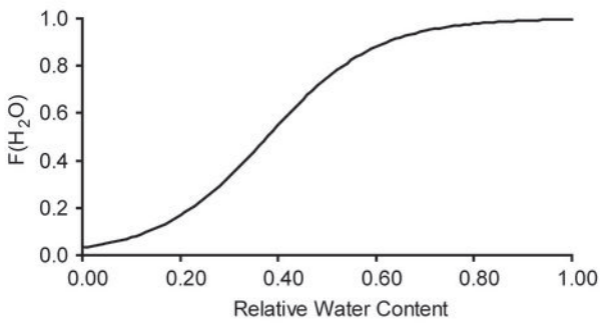
Surface Roots



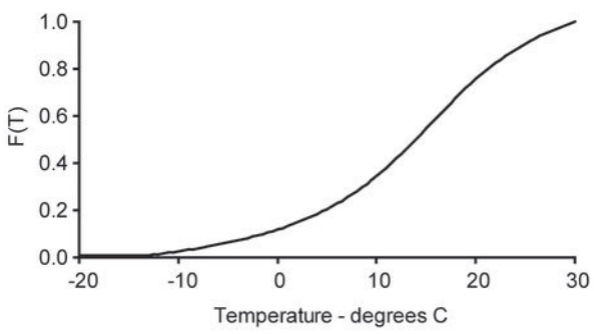
Soil Roots



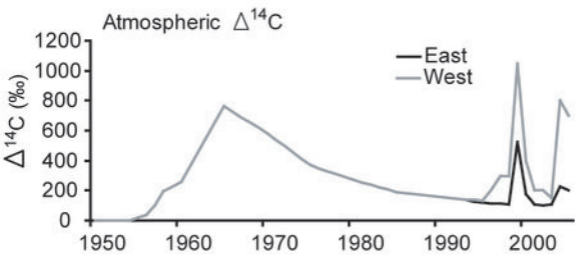
a.

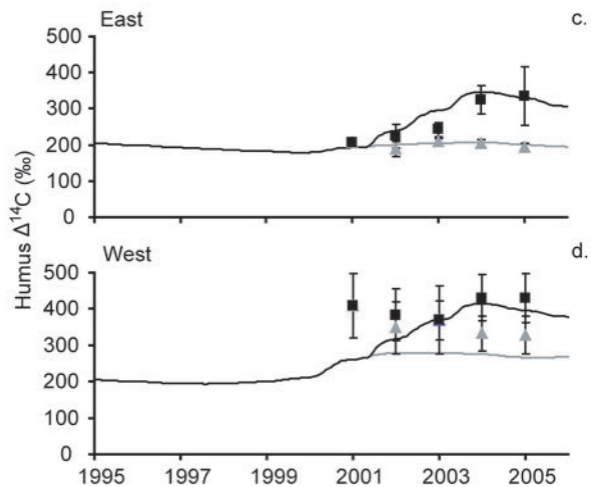
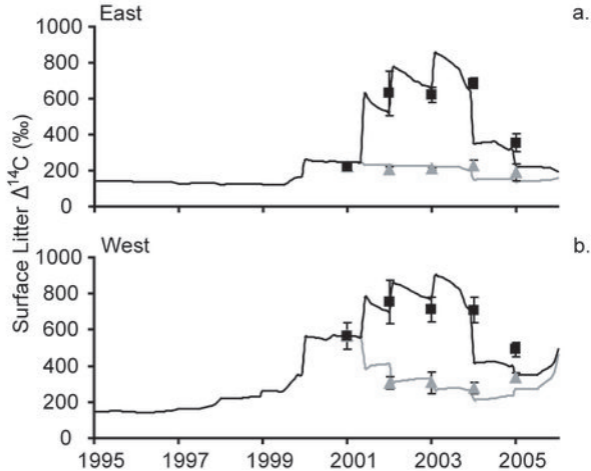


b.



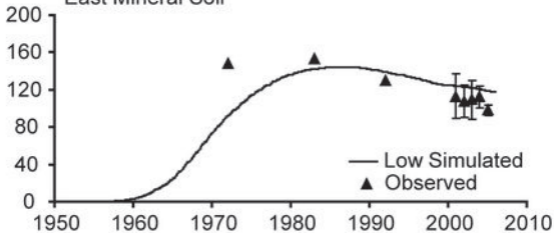
c.





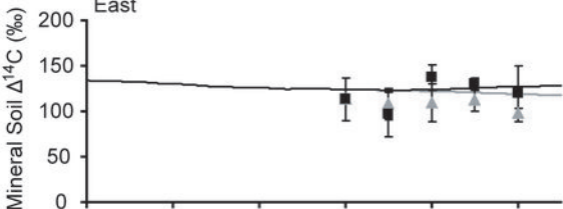
— Low Simulated — High Simulated
 ▲ Low Observed ■ High Observed

East Mineral Soil



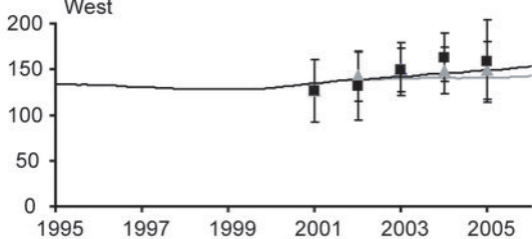
a.

East



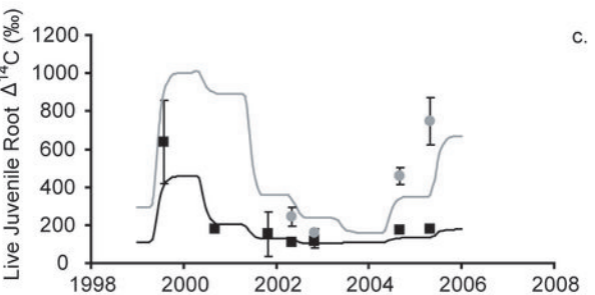
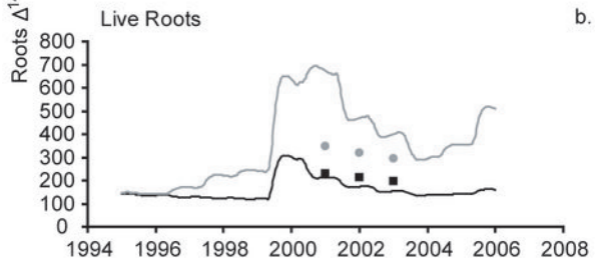
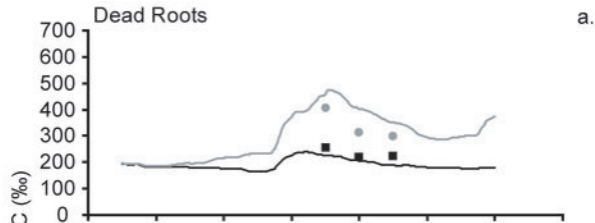
b.

West



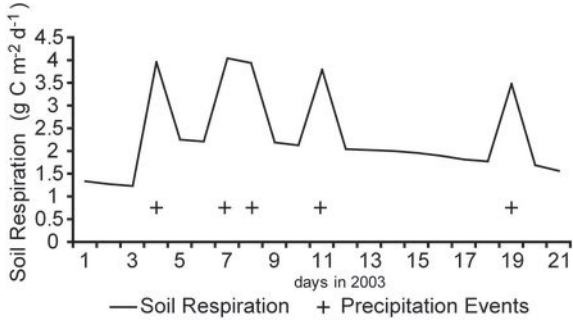
c.

— Low Simulated — High Simulated
▲ Low Observed ■ High Observed

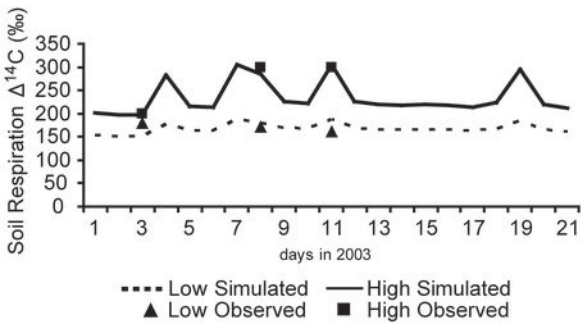


— East Simulated — West Simulated
 ■ East Observed ● West Observed

a.

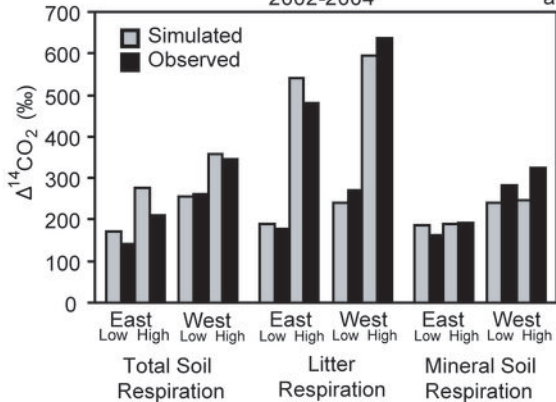


b.



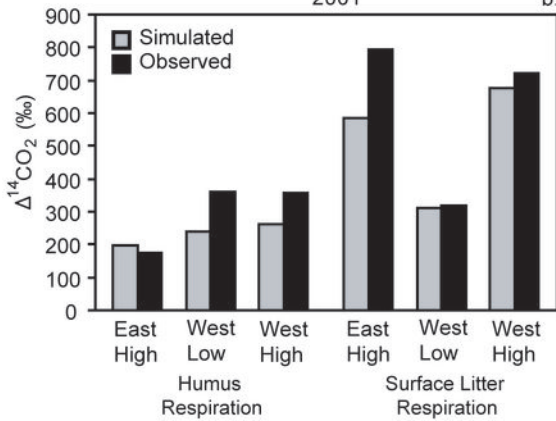
2002-2004

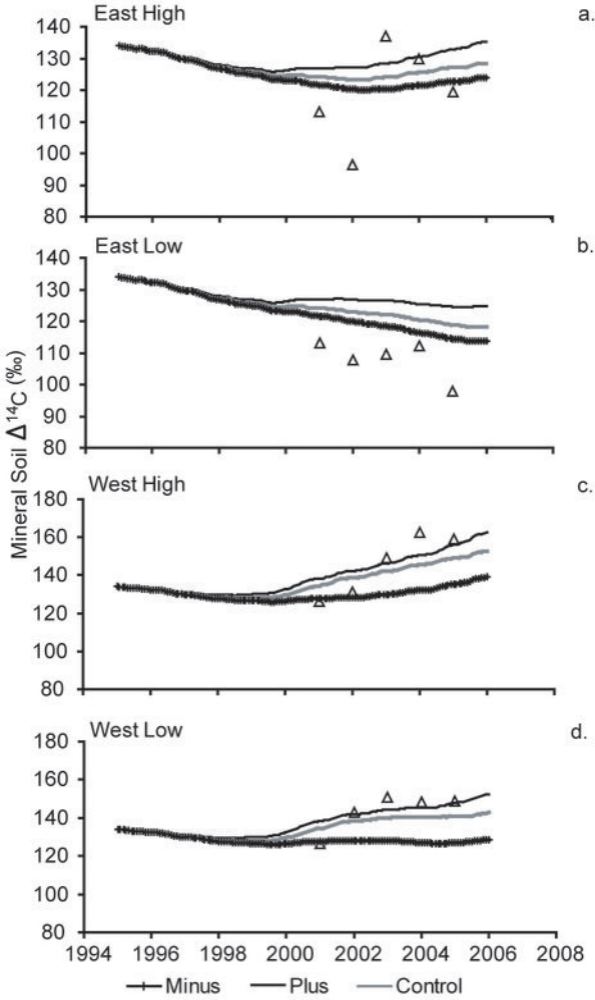
a.

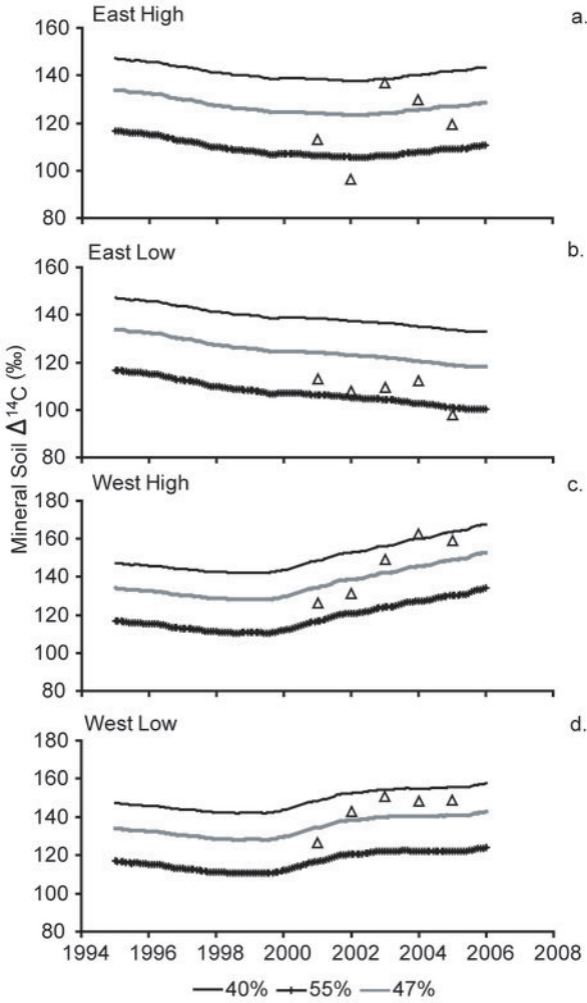


2001

b.







DISCLAIMER

This document was prepared as an account of work sponsored by the United States Government. While this document is believed to contain correct information, neither the United States Government nor any agency thereof, nor the Regents of the University of California, nor any of their employees, makes any warranty, express or implied, or assumes any legal responsibility for the accuracy, completeness, or usefulness of any information, apparatus, product, or process disclosed, or represents that its use would not infringe privately owned rights. Reference herein to any specific commercial product, process, or service by its trade name, trademark, manufacturer, or otherwise, does not necessarily constitute or imply its endorsement, recommendation, or favoring by the United States Government or any agency thereof, or the Regents of the University of California. The views and opinions of authors expressed herein do not necessarily state or reflect those of the United States Government or any agency thereof or the Regents of the University of California.